Chapter 8

Experimental Work

Laboratory thermomechanical simulation experiments were performed on a commercial steel to supplement the published data for validation of the computer model. Dilatometry and quantitative optical metallography techniques were used to follow the progress of transformation during different thermal treatments.

8.1 The Thermomechanical Simulator

The Thermecmastor-Z thermomechanical simulator, manufactured by Fujii Electronic Industrial Co. Ltd., is a laboratory machine capable of simulating a specified thermal cycle (with deformation if required) on a small specimen, under accurate computer control. The temperature and diametrical dilatation of the specimen are measured and thus the progress of phase transformations within the material can be followed.

A cylindrical specimen with dimensions 8 mm diameter $\times$ 12 mm length is placed in the Thermecmastor chamber (Figure 8.1) between two silicon nitride dies. The die holders are insulated from the dies by two mica discs. The upper die can be raised and lowered by a hydraulic ram to hold the sample in position. A platinum/platinum-10% rhodium thermocouple is spot-welded to the specimen in a central position, the contacts spaced approximately 1 mm apart. The accuracy of the temperature reading is ± 3 °C [110] whilst the variation along the specimen length is no more than ± 10 °C, the coldest region being near the dies [111]. The diametrical dilatation of the sample is monitored using a He-Ne laser beam, which moves and scans with the ram to ensure the same location on the sample is measured throughout the experiment. The beam is positioned at the same height as the thermocouple on the sample to ensure that the temperature and dilatation measurements are for the same location. The accuracy of the dilatation

reading is ± 1 μm [110]. The sealed chamber is then pumped out to a vacuum of $\approx 10^{-2}$ Pa to prevent oxidation of the specimen. An inert gas (argon) atmosphere can also be introduced if required. Heating is provided by a water-cooled, high frequency induction coil which surrounds the sample. Cooling can be controlled using gas (He or N_2) or water, He being used in all these experiments. The thermal cycle is input to a computer which then controls the operation of the program – the heating rate, gas cooling valves, etc. Time, temperature and dilatation data are recorded and can be stored on the computer for subsequent analysis.

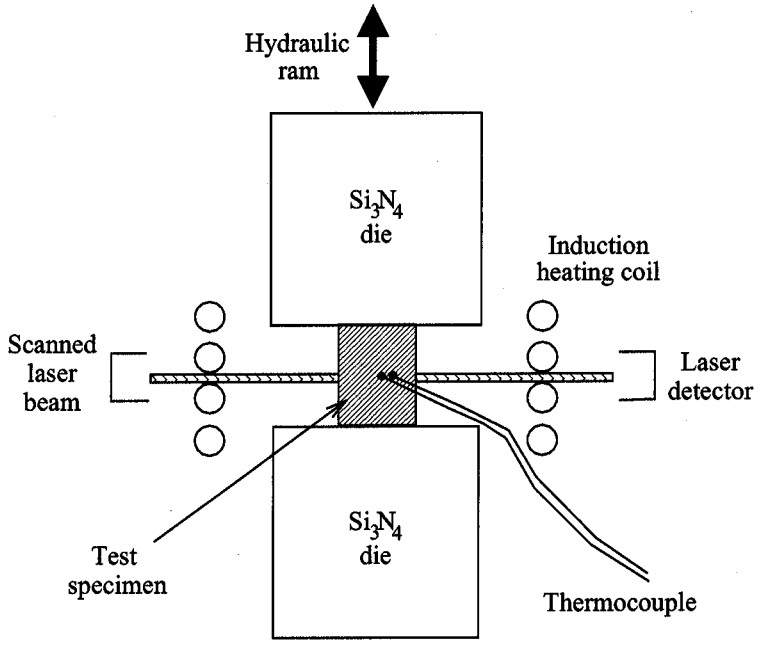

Figure 8.1: Schematic layout of the vacuum chamber of the Thermecmastor thermomechanical simulator.

8.2 Thermal Treatments

A series of experiments was carried out to investigate the effect of varying prior austenite grain size and cooling rate on the phase transformations in the same steel. A commercially produced steel provided by British Steel was used, with composition 0.21 C 0.21 Si 0.84 Mn wt.%. Prior to machining to final dimensions, 10 mm diameter steel rods were vacuum sealed in quartz tubes back-filled with argon to 150 mm Hg pressure, placed in a furnace at 1200 °C for 3 days and then air-cooled. This was to ensure complete homogenisation of the steel composition and remove any processing effects such as banding of the microstructure. The inert gas sealing prevented oxidation and decarburisation at high temperatures. The

homogenised rods were then machined into 8 mm diameter × 12 mm length specimens.

The austenitising and cooling conditions which were employed are illustrated in Figure 8.2. Austenitising temperatures of 950, 1000 and 1200 °C were selected to generate three different austenite grain sizes prior to transformation. Specimens were heated at 200 °C/min and held for 3 minutes at 950 °C or 5 minutes at the other temperatures. Specimens were cooled at 1 °C s^{-1} from each austenitising temperature, and the 1000 °C samples were additionally cooled at 0.2 and 5 °C s^{-1}. The first run for each grain size/cooling rate combination was cooled fully to room temperature. The dilatation curve was then analysed to determine suitable quench-out temperatures at which to investigate the progress of transformation (Figure 8.3). Several further runs quenched out with helium gas from these temperatures were then performed for each combination.

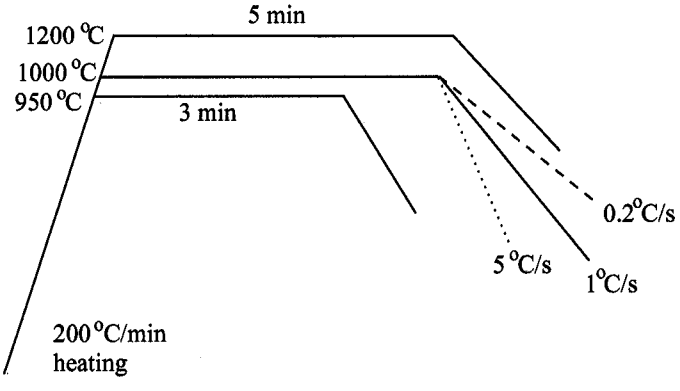

Figure 8.2: Schematic illustration of austenitising and cooling conditions for thermomechanical simulation experiments.

8.3 Experimental Results

8.3.1 Dilatation Curves

The progress of the austenite → ferrite transformation during cooling from the austenitising temperature can be followed *via* the diametrical dilatation of the specimen. As the sample is cooled from the austenite field, it starts to contract linearly with temperature, according to the thermal expansion coefficient of the austenite. When the transformation to ferrite starts, the dilatation curve begins to deviate from this line. This point can be used to determine the Ar_3 temperature for the transformation. The change in crystal structure from face-centred cubic (fcc) to body-centred cubic (bcc) causes an expansion

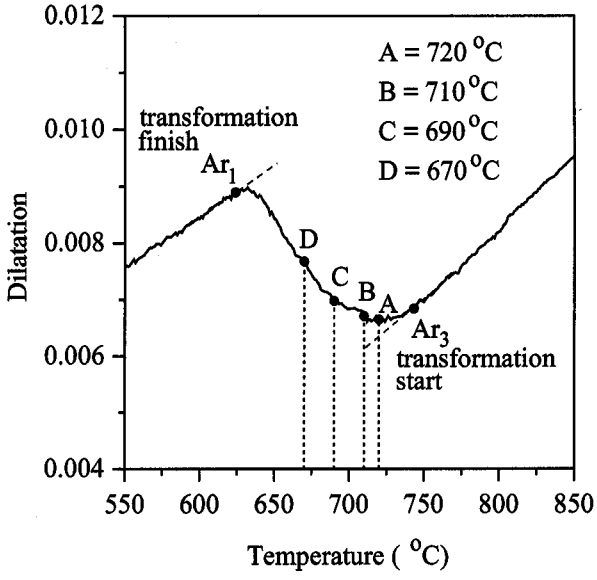

Figure 8.3: Dilatation curve for 950 °C austenitisation temperature followed by 1 °C s^{-1} cooling showing quench-out temperatures during transformation.

effect which competes with the thermal contraction. This expansion will increase with the fraction of bcc phase, until all the austenite is transformed. The curve then resumes its linear form, following the thermal expansion coefficient of the ferrite, which differs from that of the austenite and thus produces a line of different gradient.

Figure 8.4 illustrates the effect of different austenitising temperatures and cooling rates on the full transformation curve. The curves for austenitisation at 950 and 1000 °C are quite similar, which is a consequence of their similar austenite grain sizes. Austenitisation at 1200 °C resulted in a grain size several times larger and thus the start of transformation was retarded accordingly. The dilatation curves for different cooling rates from the same austenite state (5 minutes at 1000 °C) show that increasing the cooling rate suppresses both the ferrite start and finish temperatures.

A series of dilatation curves for the 1000 °C austenitising temperature and 1 °C s^{-1} cooling rate are presented in Figure 8.5. The first curve shows the full cooling curve to room temperature. Subsequent curves illustrate the quench-outs at progressively earlier stages of transformation, and have been translated parallel to the y-axis for clarity. Superposition of the 5 curves reveals that the start temperatures are identical in each case, indicating the reproducibility of the experiments.

The transformation-start and finish temperatures as measured from the dilatation curves are shown in Table 8.1 and plotted in Figure 8.6. Both the Ar_3 and Ar_1 temperatures increase with a decrease in cooling rate or austenitising temperature (grain size).

The Ar_3 is more strongly affected in both cases.

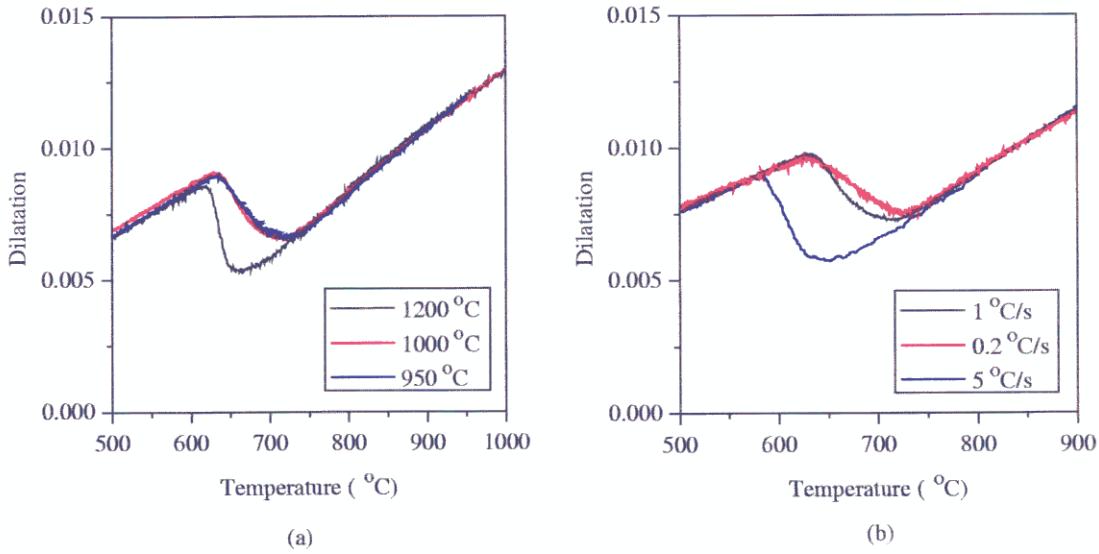

Figure 8.4: Measured dilatation curves for a 0.2 wt.% C steel illustrating the effect on the austenite to ferrite transformation of (a) austenitising temperature at a cooling rate of 1 °C s^{-1}, (b) cooling rate variations for austenitisation at 1000 °C.

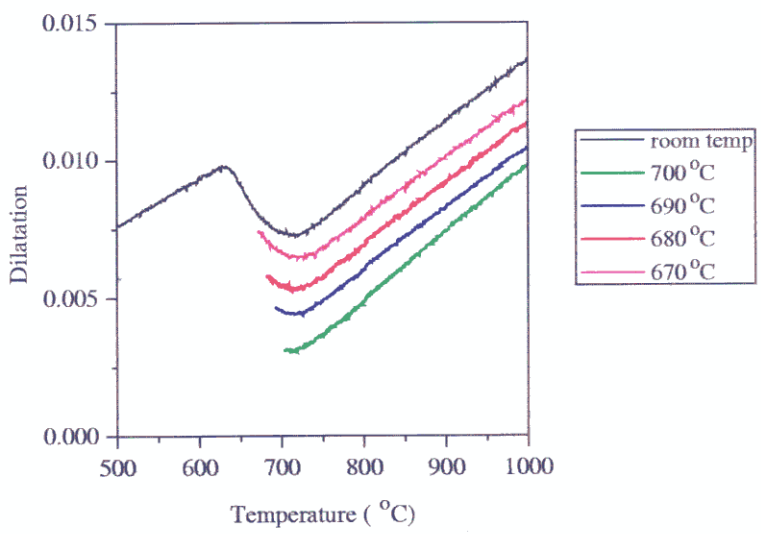

Figure 8.5: Measured dilatation curves for a 0.2 wt.% C steel austenitised at 1000 °C, cooled at 1 °C s^{-1}, and quenched out at different temperatures.

T_γ (°C)	Cooling rate (°C s^{-1})	Ar_3 (°C)	Ar_1 (°C)
950	1	750	625
1000	0.2	750	625
1000	1	730	620
1000	5	680	580
1200	1	695	610

Table 8.1: Measured austenite/ferrite transformation-start (Ar_3) and finish (Ar_1) temperatures from dilatation curves.

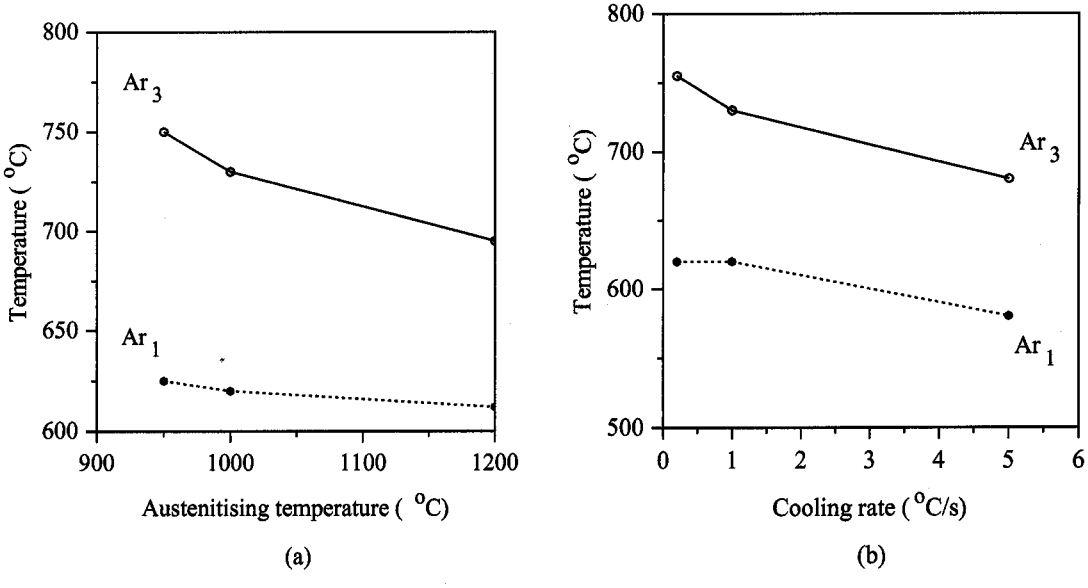

Figure 8.6: Measured variation of dilatometric transformation start and finish temperatures as a function of (a) austenitising temperature, (b) cooling rate.

8.3.2 Quantitative Metallography

The transformed samples were sectioned transversely through the centre (thermocouple position) and hot-mounted in Bakelite. They were ground using silicon carbide papers and polished with diamond paste on cloth to a 1 μm finish. The microstructure was revealed by etching with 2% nital (20 ml of concentrated nitric acid HNO_3 in 980 ml of methanol). The etched samples were quantitatively examined at British Steel to determine the proportion of each phase (allotriomorphic ferrite, Widmanstätten ferrite, etc.) present and the equiaxed ferrite grain size where applicable. The prior austenite grain size was also measured in samples quenched during the early stages of the transformation where the austenite grain boundaries were delineated with allotriomorphic ferrite. Grain sizes were measured by the lineal intercept technique in accordance with ASTM E112-88 section 11 [112]. Five separate and randomly selected fields were measured through fifty grain boundaries in all samples except those austenitised at 1200 °C, where 10 fields were measured through 15 boundaries due to the large austenite grain size. The 95% confidence limit for each sample was calculated from the standard deviation of the measurements using the procedure in ASTM E112-88 section 13. The volume fractions and their 95% confidence limits were determined by point counting in accordance with ASTM E562-83 [112]. The results are tabulated in Table 8.2.

The variation of austenite grain size with austenitising temperature is plotted in Figure 8.7. The grain size increased from around 100 μm at 950 °C to over 400 μm at 1200 °C. The eleven different austenite grain size measurements for 1000 °C ranged from 126 to 152 μm, showing reasonable consistency between experiments.

Figure 8.8 shows the evolution of the allotriomorphic ferrite grain size during cooling from four different austenitic states. In each case, the average ferrite grain size increased as the transformation progressed. Ferrite nuclei formed early in the transformation continued to grow until transformation was complete. The final ferrite grain size decreased as cooling rate increased for the same austenite grain size, or as austenite grain size decreased for the same cooling rate. The largest ferrite grains were produced by cooling from 1000 °C at 0.2 °C s^{-1}, whilst the smallest resulted from 5 °C s^{-1} cooling from the same temperature. A small austenite grain size generates a high nucleation rate due to the larger number of potential nucleation sites it provides per unit volume. The grains will therefore be smaller in size when they impinge and cease growing. Fast cooling produces a high nucleation rate and provides little time for growth, so the final grain size is also small. Slow cooling rates provide a smaller driving force for nucleation and a correspondingly lower nucleation rate. There is also more time available for growth so the grains are much larger upon impingement.

Figure 8.9 illustrates the variation in volume fraction of equiaxed (allotriomorphic) ferrite and Widmanstätten ferrite with cooling rate and austenite grain size. It can be seen that an increase in austenitising temperature, T_γ, and thus in austenite grain size, led to a decrease in equiaxed ferrite fraction and an increase in Widmanstätten ferrite. A larger grain size decreases the amount of boundary area per unit volume, which is the predominant nucleation site for allotriomorphic ferrite. It also reduces the possibility of early impingement of particles growing from opposite sides of the austenite grains, thus enabling the fast-growing Widmanstätten ferrite plates to dominate the microstructure. An increase in the cooling rate also produces a decrease in allotriomorphic ferrite fraction, as the ferrite-start temperature is suppressed. The temperature is rapidly reduced to where allotriomorphic ferrite growth slows down, allowing Widmanstätten ferrite to dominate.

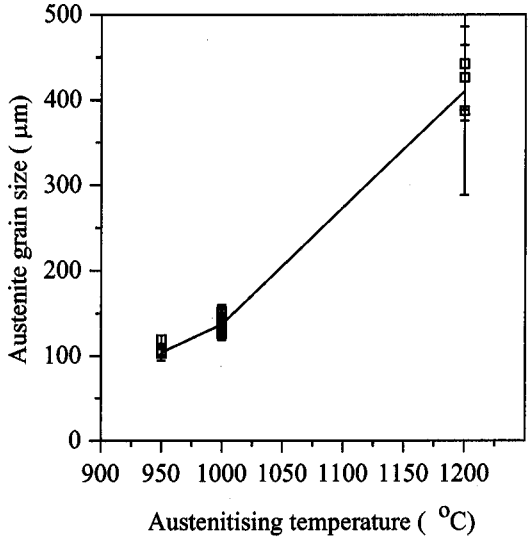

Figure 8.7: Measured variation in austenite grain size with austenitising temperature in a 0.2 wt.% C steel.

8.3.3 Optical Micrographs

Optical micrographs were taken of representative areas of the etched samples, and a selection of these are presented in Figures 8.10 through 8.19. The progress of the transformation for each set of austenitisation and cooling conditions, as plotted quantitatively in Figure 8.9, can be seen in the micrographs as follows: 1200 °C, 1 °C s^{-1} – Figure 8.10; 1000 °C, 1 °C s^{-1} – Figure 8.11 - 8.13; 950 °C, 1 °C s^{-1} – Figure 8.14 - 8.15; 1000 °C, 0.2 °C s^{-1} – Figure 8.16 - 8.18a; and 1000 °C, 5 °C s^{-1} – Figure 8.18b - 8.19. In each case, the fractions of allotriomorphic ferrite and Widmanstätten ferrite increased as the quench

T_γ (°C)	t_γ (min)	d_γ (μm)	CR (°C/s)	T_q (°C)	EF (%)	WF (%)	P (%)	FS (%)	M (%)	d_α (μm)
1200	5	443±67	1	–	13±3	39±5	46±5	3±2	0	–
1200	5	427±38	1	650	12±3	29±5	30±4	11±3	18±5	–
1200	5	387±99	1	670	10±3	7±2	11±3	3±2	69±5	–
1000	5	150±6	1	–	41±4	33±4	25±4	1±1	0	20±3
1000	5	138±6	1	670	41±4	15±4	21±4	0	23±4	20±3
1000	5	152±8	1	680	31±4	13±4	14±3	0	41±4	18±2
1000	5	132±6	1	690	22±4	5±2	12±3	2±2	59±5	17±2
1000	5	146±9	1	700	12±3	5±2	12±3	4±1	67±5	15±1
950	3	–	1	–	66±4	14±4	18±3	2±1	0	16±1
950	3	–	1	670	43±5	7±3	37±5	2±1	11±3	15±1
950	3	106±7	1	690	38±5	6±2	46±5	2±1	8±3	14±1
950	3	103±9	1	710	26±4	3±2	39±5	10±3	21±4	15±2
950	3	119±5	1	720	9±3	26±4	29±5	2±2	33±6	11±1
1000	5	127±1	5	–	17±3	32±4	49±5	2±1	0	11±2
1000	5	126±5	5	610	14±4	31±4	51±4	2±1	2±1	10±1
1000	5	130±11	5	620	14±3	31±4	52±4	1±1	1±1	9±1
1000	5	137±9	5	630	12±3	22±4	44±5	4±2	17±4	11±1
1000	5	–	0.2	300	71±4	1±1	29±4	0	0	24±2
1000	5	–	0.2	700	49±4	2±1	9±2	2±3	37±4	22±3
1000	5	–	0.2	710	53±4	1±1	14±3	1±1	31±4	24±1
1000	5	136±8	0.2	720	31±5	1±1	14±3	2±1	53±4	20±1
1000	5	142±7	0.2	730	14±3	3±2	13±3	9±3	62±5	16±3

Table 8.2: Quantitative metallographic results for thermomechanical simulation experiments. T_γ = austenitising temperature, t_γ = austenitising time, d_γ = austenite grain size, CR = cooling rate, T_q = quench temperature, EF = equiaxed (allotriomorphic) ferrite, WF = Widmanstätten ferrite, P = pearlite, FS = ferrite sideplates (bainite), M = martensite, d_α = ferrite grain size. Grain sizes are reported to the nearest 1 μm, volume fractions to the nearest 1%. 95% confidence limits are quoted for all measurements.

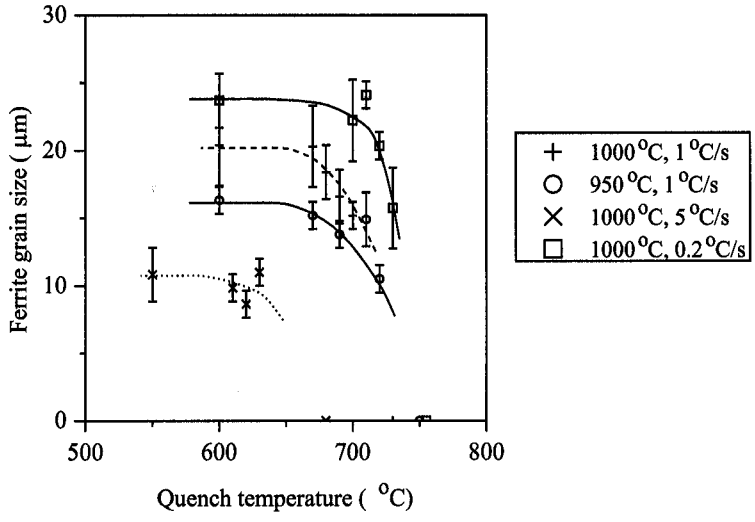

Figure 8.8: Measured evolution of ferrite grain size with temperature during cooling in a 0.2 wt.% C steel.

temperature decreased. In all the experiments the first transformation occurred at the prior austenite grain boundaries (Figures 8.11a, 8.14a, 8.16a and 8.19a). Allotriomorphic ferrite was usually the first phase to form, but at the largest austenite grain size (1200 °C austenitising temperature) and the fastest cooling rate (5 °C s^{-1}), a significant amount of Widmanstätten ferrite was also observed at the highest quench temperatures, close to the Ar_3 (Figure 8.10a). In both these cases, the allotriomorphic ferrite transformation was suppressed, either by the reduced amount of grain boundary area per unit volume or the decrease in growth kinetics as the temperature fell rapidly. In the other experiments, similar undercoolings of 25 to 30 °C below the Ar_3 produced much smaller proportions of Widmanstätten ferrite (Figures 8.14 and 8.16) in comparison with allotriomorphic ferrite.

8.3.4 Summary

Laboratory thermomechanical simulation experiments were carried out on a commercial steel to provide data with which to validate the theoretical phase transformation models. The progress of austenite transformation under several austenitising and cooling schedules was followed using dilatometry and optical metallography. Quantitative analysis of the specimens produced information on the volume fraction of each phase formed and the allotriomorphic ferrite grain size. The increase in the proportion of Widmanstätten ferrite at the expense of allotriomorphic ferrite, as both austenite grain size and cooling rate increased, is consistent with published experimental work [15, 127].

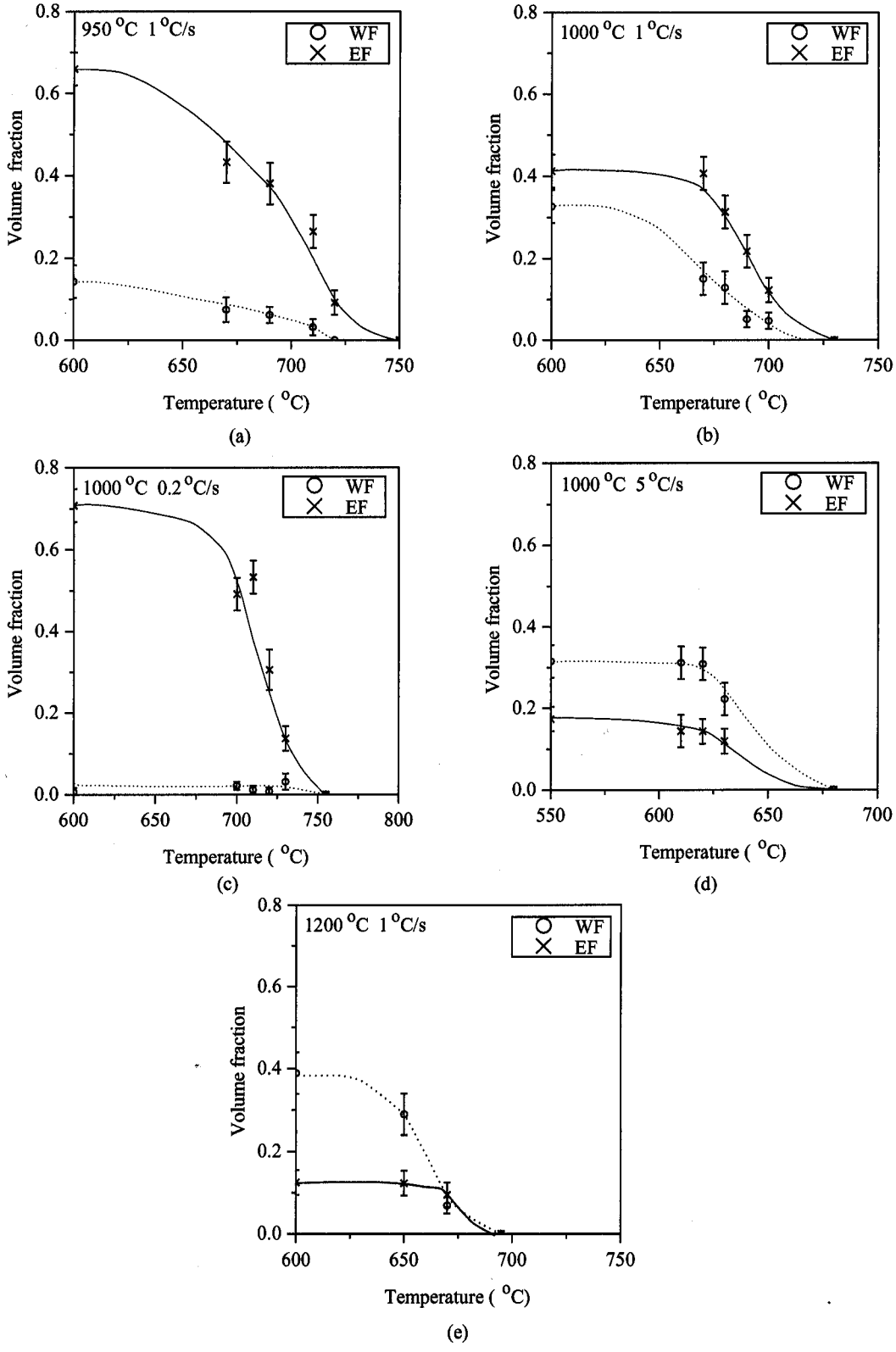

Figure 8.9: Measured volume fractions of equiaxed and Widmanstätten ferrite as a function of temperature in a 0.2 wt.% C steel for (a) $T_\gamma = 950$ °C, CR = 1 °C s^{-1}, (b) $T_\gamma = 1000$ °C, CR = 1 °C s^{-1}, (c) $T_\gamma = 1000$ °C, CR = 0.2 °C s^{-1}, (d) $T_\gamma = 1000$ °C, CR = 5 °C s^{-1}, (e) $T_\gamma = 1200$ °C, CR = 1 °C s^{-1}.

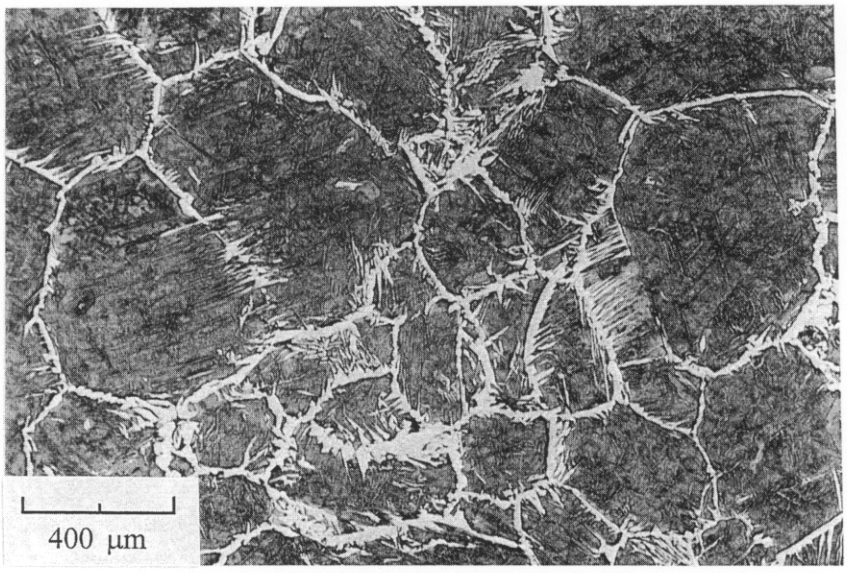

(a)

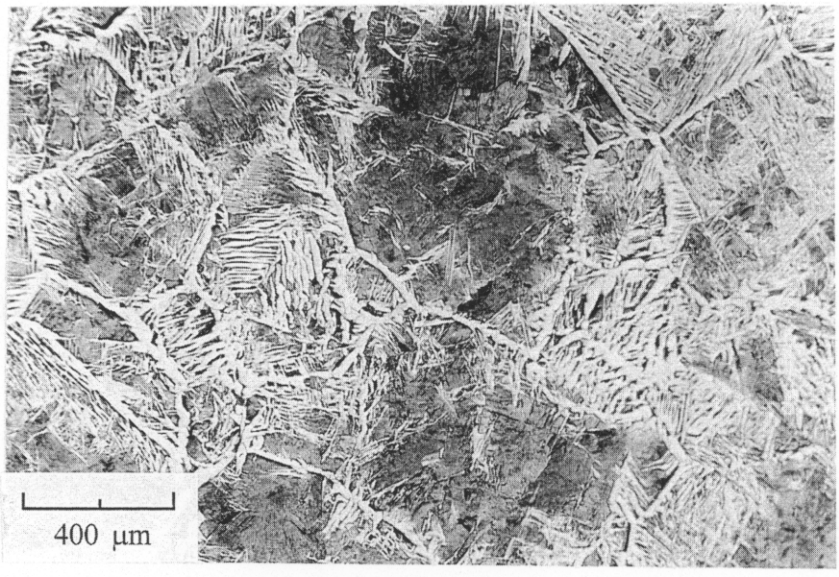

(b)

Figure 8.10: Optical micrographs of a 0.2 wt.% C steel, austenitised at 1200 °C and cooled at 1 °C s^{-1}, (a) quenched from 670 °C, showing ferrite decorating the prior austenite grain boundaries, (b) cooled to room temperature, with large amounts of Widmanstätten ferrite.

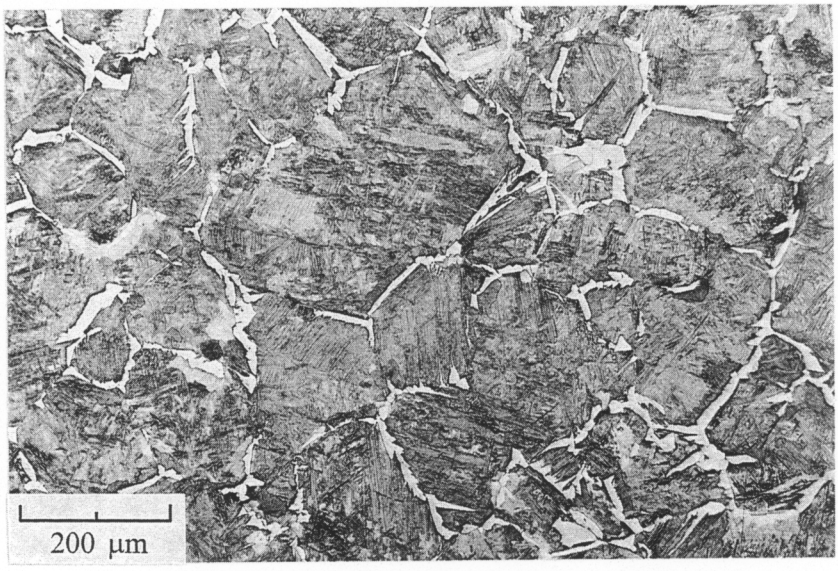

(a)

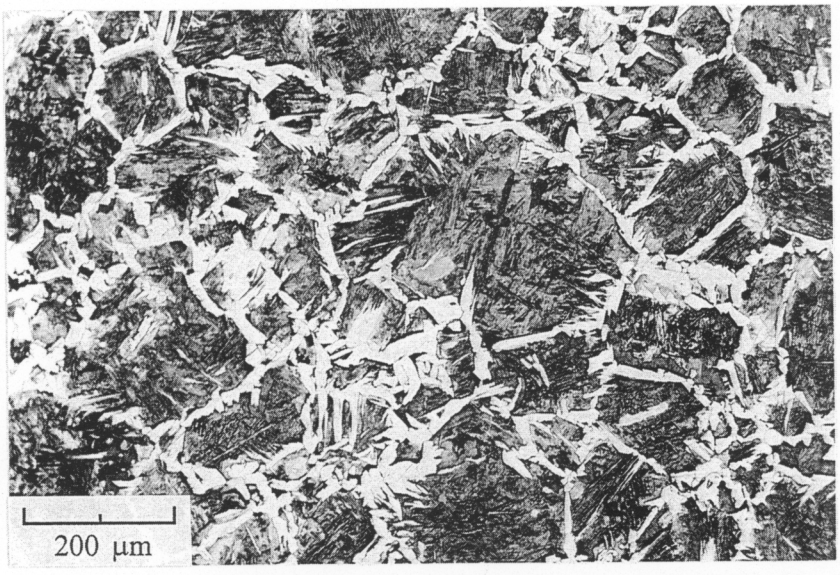

(b)

Figure 8.11: Optical micrographs of a 0.2 wt.% C steel, austenitised at 1000 °C and cooled at 1 °C s^{-1}, (a) quenched from 700 °C, (b) quenched from 690 °C.

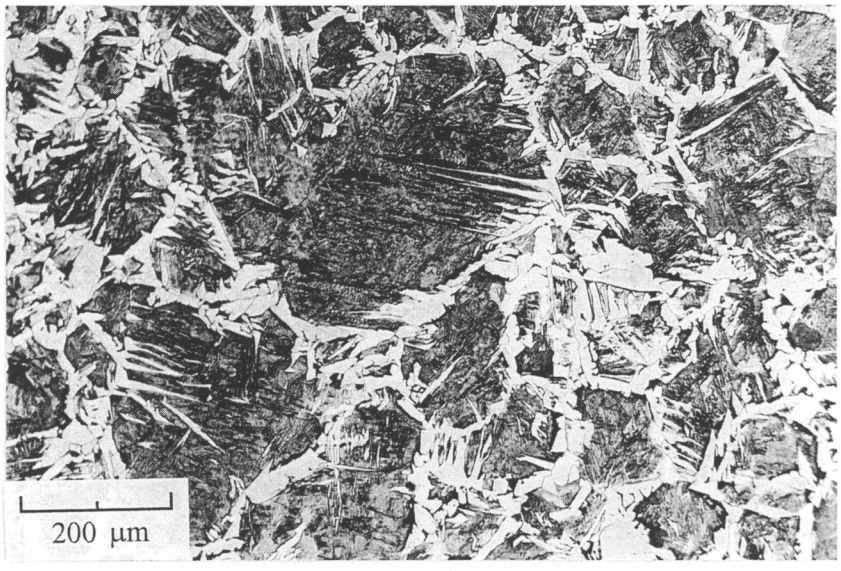

(a)

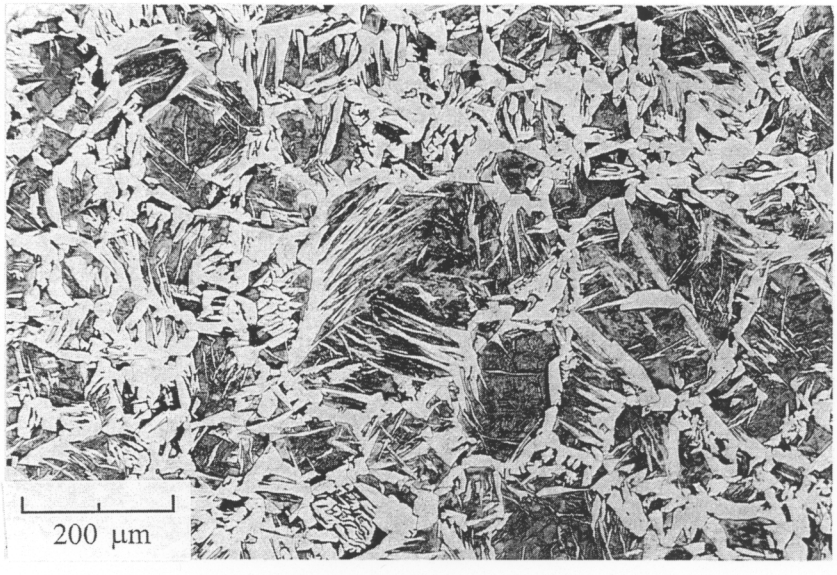

(b)

Figure 8.12: Optical micrographs of a 0.2 wt.% C steel, austenitised at 1000 °C and cooled at 1 °C s^{-1}, (a) quenched from 680 °C, (b) quenched from 670 °C.

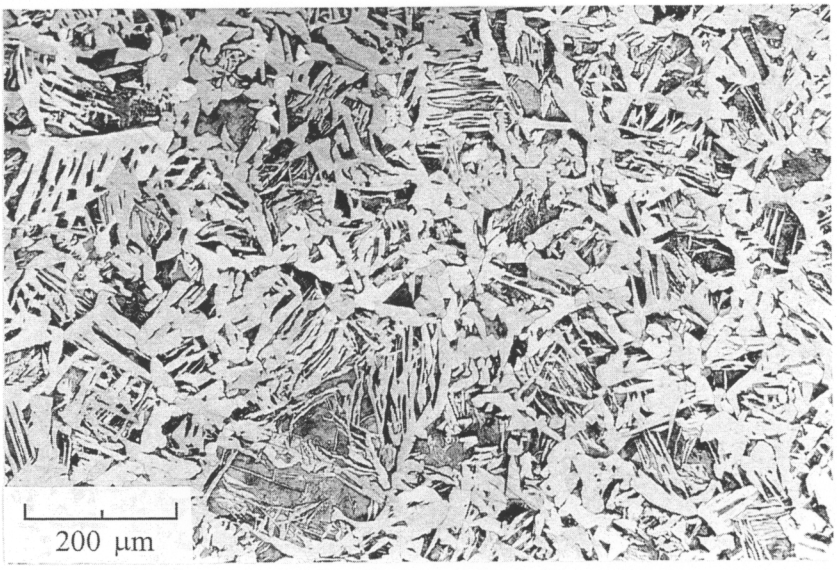

Figure 8.13: Optical micrograph of a 0.2 wt.% C steel, austenitised at 1000 °C and cooled at 1 °C s^{-1} to room temperature, showing the mixture of allotriomorphic ferrite, Widmanstätten ferrite and pearlite in the microstructure.

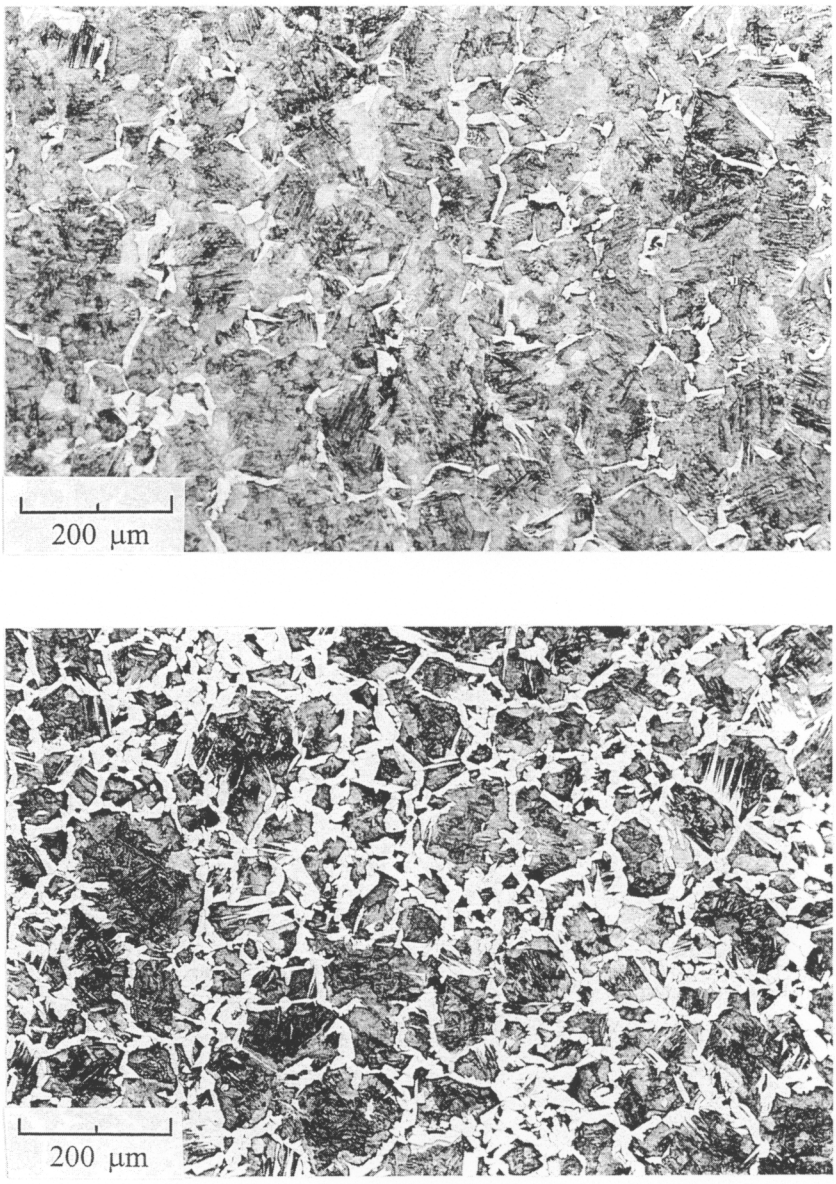

(a)

(b)

Figure 8.14: Optical micrographs of a 0.2 wt.% C steel, austenitised at 950 °C and cooled at 1 °C s^{-1}, (a) quenched from 720 °C, (b) quenched from 710 °C.

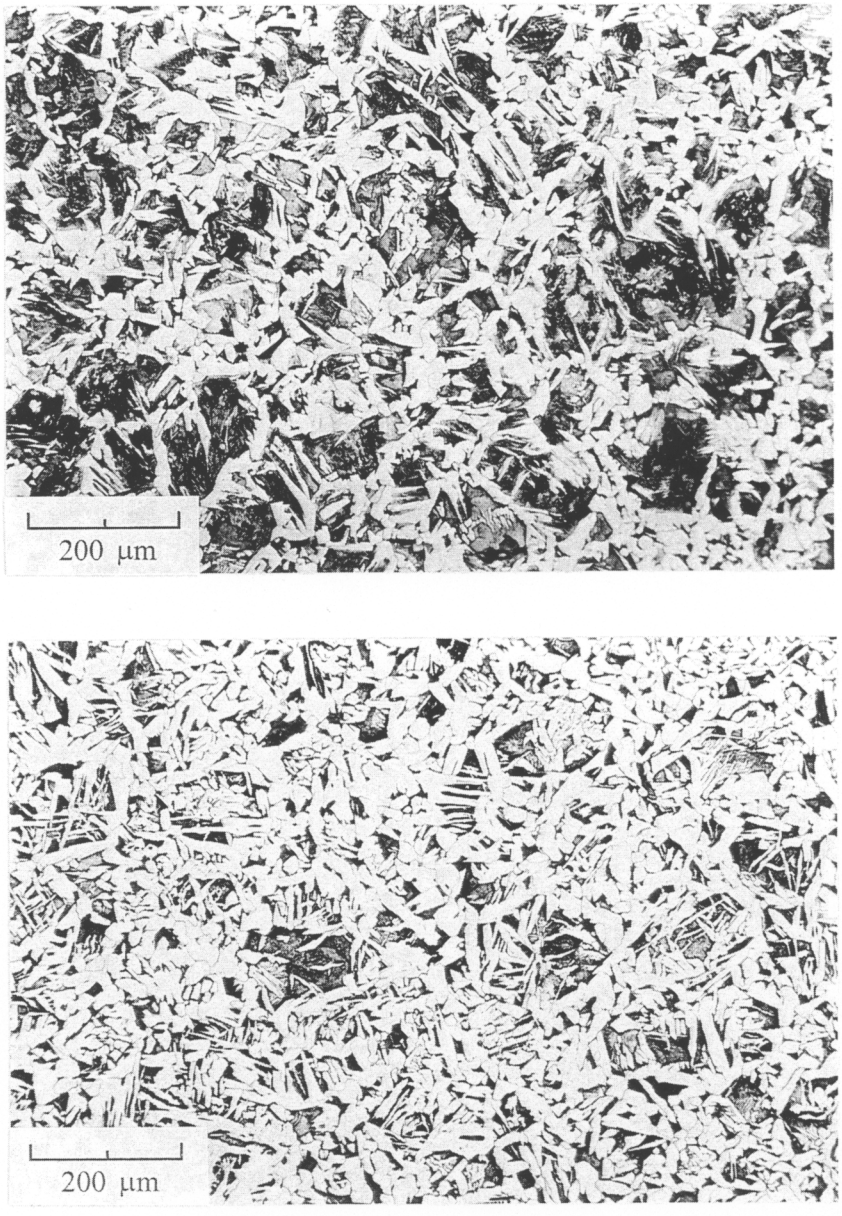

(a)

(b)

Figure 8.15: Optical micrographs of a 0.2 wt.% C steel, austenitised at 950 °C and cooled at 1 °C s^{-1}, (a) quenched from 670 °C, (b) cooled to room temperature.

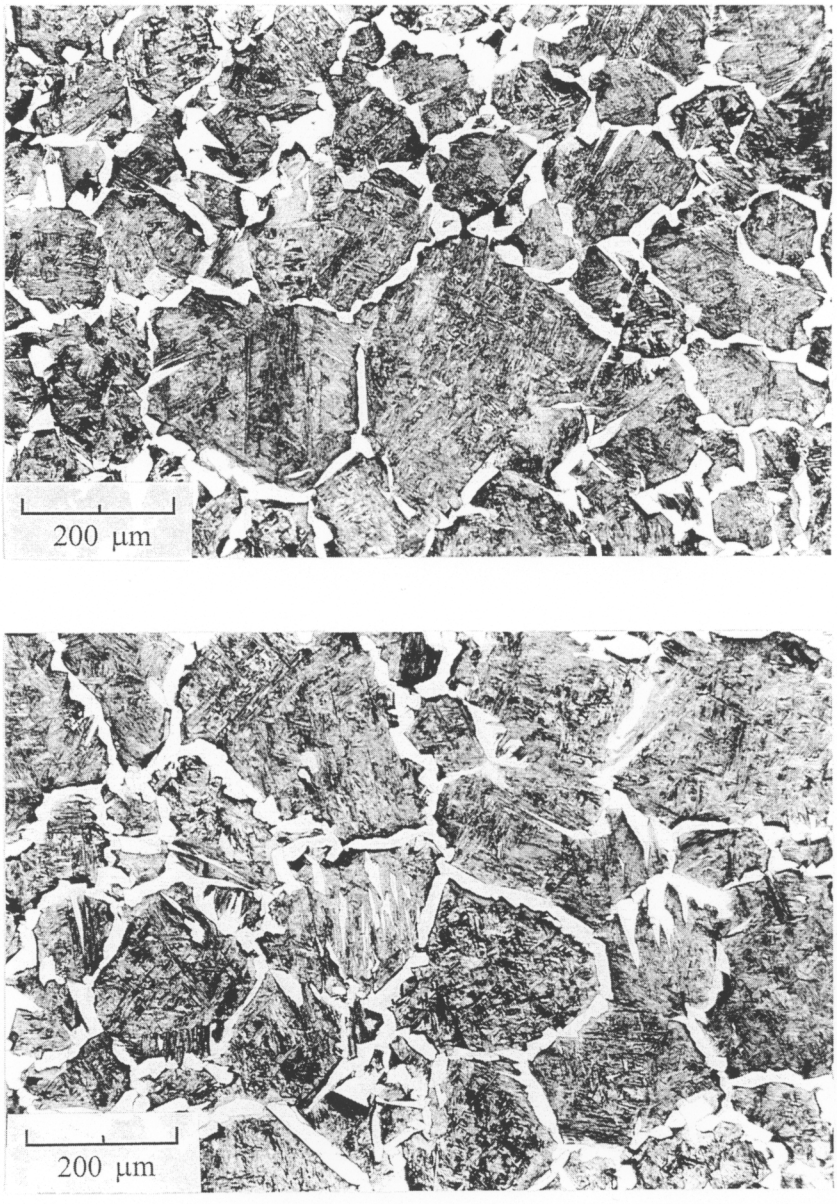

(a)

(b)

Figure 8.16: Optical micrographs of a 0.2 wt.% C steel, austenitised at 1000 °C and cooled at 0.2 °C s^{-1}, (a) quenched from 730 °C, (b) quenched from 720 °C.

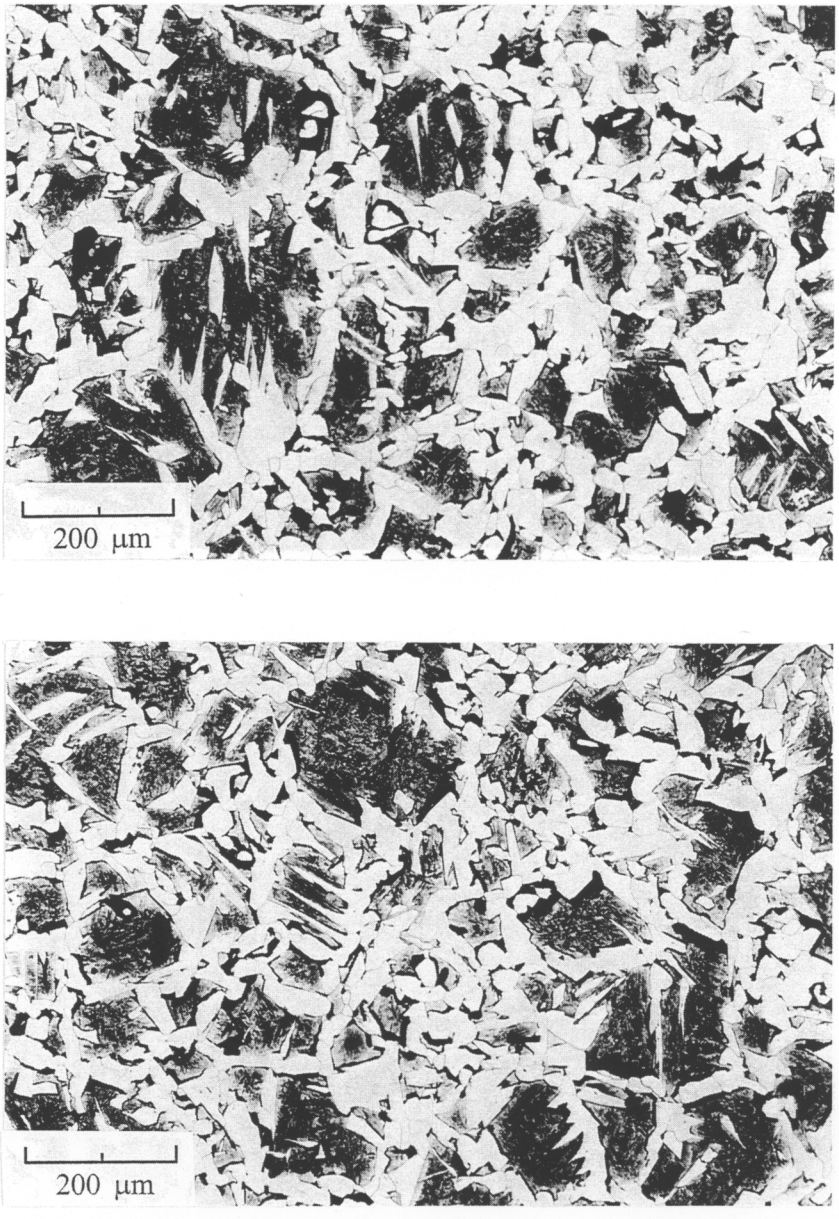

(a)

(b)

Figure 8.17: Optical micrographs of a 0.2 wt.% C steel, austenitised at 1000 °C and cooled at 0.2 °C s^{-1}, (a) quenched from 710 °C, (b) quenched from 700 °C.

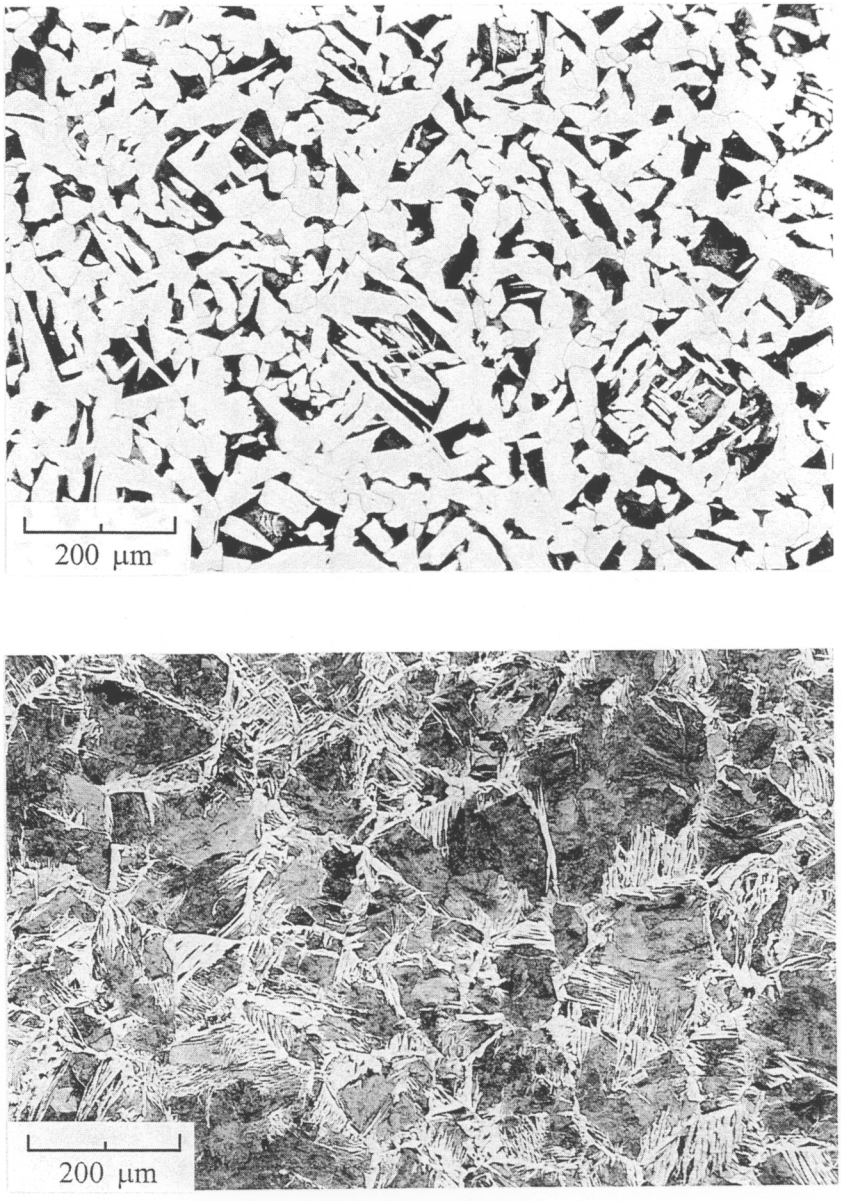

(a)

(b)

Figure 8.18: Optical micrographs of a 0.2 wt.% C steel, austenitised at 1000 °C and cooled to room temperature at (a) 0.2 °C s^{-1}, showing the microstructure of predominantly allotriomorphic ferrite, (b) 5 °C s^{-1}.

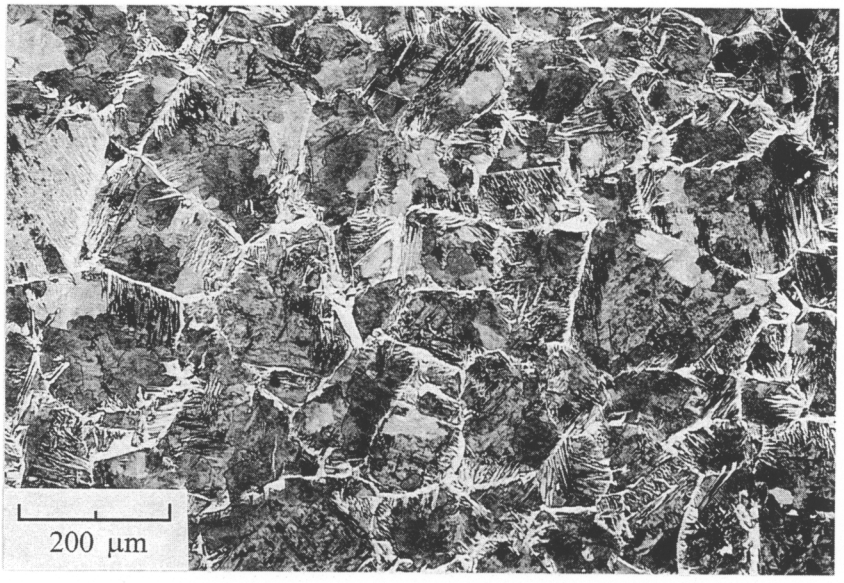

(a)

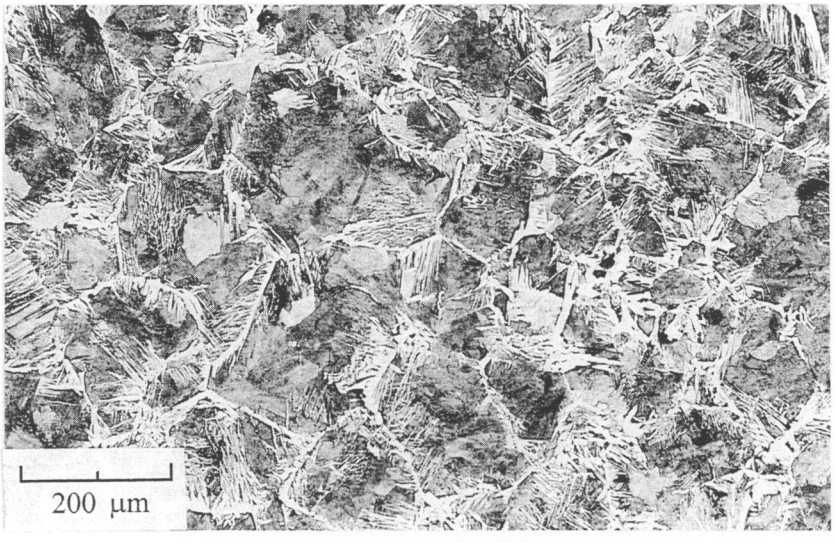

(b)

Figure 8.19: Optical micrographs of a 0.2 wt.% C steel, austenitised at 1000 °C and cooled at 5 °C s^{-1}, (a) quenched from 630 °C, (b) quenched from 610 °C.